

# Video Quality Assessment and Coding Complexity of the Versatile Video Coding Standard

Thomas Amestoy, Naty Sidaty, Wassim Hamidouche, Pierrick Philippe and Daniel Menard

**Abstract**—In recent years, the proliferation of multimedia applications and formats, such as IPTV, Virtual Reality (VR, 360°), and point cloud videos, has presented new challenges to the video compression research community. Simultaneously, there has been a growing demand from users for higher resolutions and improved visual quality. To further enhance coding efficiency, a new video coding standard, Versatile Video Coding (VVC), was introduced in July 2020. This paper conducts a comprehensive analysis of coding performance and complexity for the latest VVC standard in comparison to its predecessor, High Efficiency Video Coding (HEVC). The study employs a diverse set of test sequences, covering both High Definition (HD) and Ultra High Definition (UHD) resolutions, and spans a wide range of bit-rates. These sequences are encoded using the reference software encoders of HEVC (HM) and VVC (VTM). The results consistently demonstrate that VVC outperforms HEVC, achieving bit-rate savings of up to 40% on the subjective quality scale, particularly at realistic bit-rates and quality levels. Objective quality metrics, including PSNR, SSIM, and VMAF, support these findings, revealing bit-rate savings ranging from 31% to 40%, depending on the video content, spatial resolution, and the selected quality metric. However, these improvements in coding efficiency come at the cost of significantly increased computational complexity. On average, our results indicate that the VVC decoding process is 1.5 times more complex, while the encoding process becomes at least eight times more complex than that of the HEVC reference encoder. Our simultaneous profiling of the two standards sheds light on the primary evolutionary differences between them and highlights the specific stages responsible for the observed increase in complexity.

**Index Terms**—VVC, HEVC, Complexity analyses, Quality assessments, Future video coding, Gains.

## I. INTRODUCTION

OVER the last decade, there has been a significant surge in multimedia services and video applications, driven by remarkable advancements in digital technologies. Emerging video applications and image representations offer a more immersive and natural viewing experience. However, these new services demand higher quality and resolution, such as 4K and 8K, to meet the quality of service expectations of end users. The widely recognized video coding standard, High Efficiency Video Coding (HEVC)/H.265, has gradually gained adoption in numerous application systems. It offers up to a 50% reduction in bit-rate while maintaining equal subjective quality compared to its predecessor, Advanced Video Coding (AVC)/H.264 standard [1]–[3]. In 2015, new coding tools were

developed under the Joint Exploration Model (JEM) software, aiming to achieve substantial bit-rate savings compared to the HEVC standard, and promising results were obtained [4], [5]. However, these quality improvements have introduced a significant increase in complexity [4].

To address these challenges, the Joint Video Experts Team (JVET) issued a call for proposals in 2017 to develop a new video coding standard, initially known as Beyond the HEVC or Future Video Coding (FVC), now referred to as Versatile Video Coding (VVC)/H.266 [6], [7]. VVC is poised to facilitate the deployment of higher-quality video services and emerging applications, including High Dynamic Range (HDR), High Frame Rate (HFR), and 360-degree omnidirectional immersive multimedia. Completed in July 2020, the primary goal of VVC/H.266 is to achieve a substantial improvement in compression performance compared to the existing HEVC/H.265 standard. The aim is to achieve a bit-rate savings of 40% or more in terms of Peak Signal to Noise Ratio (PSNR) compared to HEVC, with a reasonable increase in complexity at both the encoder and decoder. The new standard is anticipated to enable the delivery of Ultra High Definition (4K) and 8K services at bit-rates comparable to those used for HDTV, effectively doubling the amount of multimedia content that can be stored on a server or transmitted through a streaming platforms. However, it is essential to note that the computational complexity and energy consumption of recent video compression standards has become a critical concern [8]. Prior research has delved into the complexity aspects of HEVC encoding/decoding for various resolutions, including High Definition (HD) (1920×1080) and Ultra High Definition (UHD) (4K) [9]–[12]. In the case of JEM tools, the coding gains achieved come at the cost of significantly increased complexity, estimated to be ten times higher for both encoder and decoder in Inter coding configuration.

In this paper, we conduct a comprehensive assessment of the emerging VVC/H.266 standard, comparing it to the established HEVC/H.265 standard. This evaluation encompasses both subjective and objective quality analyses. We utilize the VVC reference software model (VTM) and compare it with the HEVC reference software model (HM) in Random Access (RA) coding configuration. Our study encompasses a diverse set of video content, spanning various bit-rates and two spatial resolutions: HD and UHD [13]. Additionally, this paper offers an in-depth analysis of time and complexity distributions for both the encoding and decoding processes. To elucidate the principal evolution from one reference software to the other, we concurrently present the profiling of VTM-5.0 and HM-16.20. While a previous study [11] assessed the impact of

N. Sidaty, T. Amestoy, W. Hamidouche and D. Menard were with with Univ. Rennes, INSA Rennes, CNRS, IETR - UMR 6164, Rennes, France, (e-mail: [thomas.amestoy@insa-rennes.fr](mailto:thomas.amestoy@insa-rennes.fr) and [wassim.hamidouche@insa-rennes.fr](mailto:wassim.hamidouche@insa-rennes.fr))

P. Philippe was with Orange Lab, 1219 Avenue des Champs Blancs, 35510 Cesson-Sévigné, France, e-mails: ([pierrick.philippe@orange.com](mailto:pierrick.philippe@orange.com))

specific new tools on VVC/H.266 complexity by disabling them individually and measuring encoding/decoding times, it is crucial to note that many other tools are mandatory in the primary profile and cannot be disabled on the encoder side. Furthermore, disabling a single tool can lead to different coding decisions compared to the reference configuration. The profiling approach employed in our study [11] offers two significant advantages compared to the aforementioned work: it enables us to evaluate the complexity of all encoding/decoding tools comprehensively, and complexity measurements are conducted within the original encoding/decoding processes with all tools enabled.

The rest of this paper are organized as follows. Section II gives an introduction to the VVC standard, including its architecture and the key coding tools integrated into the VTM. Section III outlines our methodology for subjective quality assessment, detailing the test material, experimental environment, and the methodologies employed. The results obtained from our assessments, along with their associated analysis, are presented in Section IV. Section V offers an in-depth examination of complexity distributions for both the encoding and decoding processes. Finally, Section VI concludes the paper.

## II. VVC TOOLS DESCRIPTION

As HEVC, VVC has a block-based hybrid coding architecture, combining Inter and Intra predictions with transform coding. Based on the HEVC standard, VVC refined existing technologies but also added novel coding tools. In this section, we briefly describe the main VVC coding tools present in the VVC Test Model (VTM)-5.0 codec, including frame partitioning, Multiple Transform Selection (MTS), in-loop filtering, Intra & Inter predictions and entropy coding. Most of the potential contributions in VVC are provided by a set of tools, given in Table I, with their individual loss when these tools are disabled in the VTM-5.0. The authors do not intend here to provide an exhaustive description of the VVC tools, for detailed description of these coding tools, the reader is referred to [7], [14].

### A. Frame Partitioning

In HEVC, the Quad Tree (QT) partitioning suffered from several limitations:

- Coding Units (CUs) could only be square, with no flexible shape to cover all block characteristics.
- Luma and Chroma components of the encoded sequence have the same QT splitting which is rarely optimal for chroma.
- Residual could only be split into Transform Units (TUs) with square shapes, reducing the potential impact of transforms.

To overcome these limitations, the VTM integrates a nested recursive Multi-Type Tree (MTT) partitioning, i.e., Binary Tree (BT) and Ternary Tree (TT) splits, in addition to the recursive QT partitioning used in HEVC. Fig. 1 illustrates all available split in VTM for a  $4N \times 4N$  CU. The BT

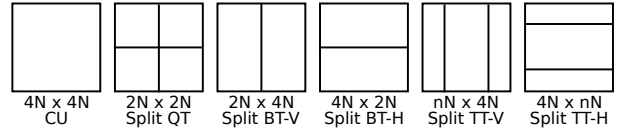


Fig. 1: Available split included in VTM-5.0 of a  $4N \times 4N$  CU.

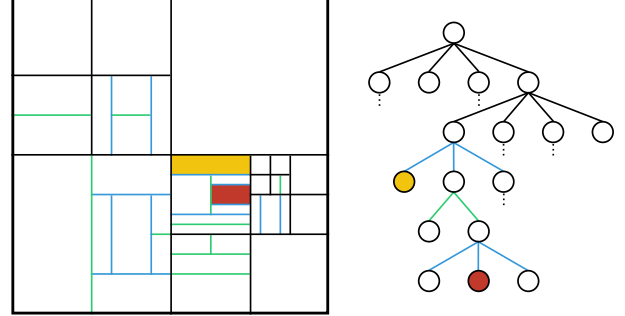


Fig. 2: Example of a CTU partitioning with a part of its corresponding tree representation.

partitioning consists of symmetric horizontal splitting (BT-H) and symmetric vertical splitting (BT-V) while the TT partitioning allows horizontal triple-tree splitting (TT-H) and vertical triple-tree splitting (TT-V) corresponding to split the CU in three blocks with the middle blocks size equal to the half of the CU. Once a BT or TT split has been executed on a CU, any further QT split is prohibited within its sub-CUs. In Figure 2, the example on the left illustrates the division of a Coding Tree Unit (CTU) into multiple CUs after the application of CTU partitioning with QT and MTT splits. The right side of the figure displays a segment of the CTU partitioning tree structure, where dark, green, and blue lines denote QT, BT, and TT splits, respectively. The yellow and red backgrounds highlight two instances of the corresponding CUs within the CTU partitioning and its related tree.

To address the limitation of square residual TUs observed in HEVC, the VTM has introduced rectangular transforms. This transformation is applied directly to the CUs, regardless of their shape, eliminating the need for any additional subdivision of residual blocks [15]. Additionally, the Intra Sub-Partitioning (ISP) tool has the capability to further split Intra-predicted blocks either vertically or horizontally into 2 or 4 sub-partitions, depending on the block size. ISP enables a bitrate saving of 0.41% in AI coding configuration.

The concept of merging TUs and CUs into a single entity is introduced. Additionally, it's noteworthy that different partition trees can be employed for the Luma and Chroma components in intra-predicted slices within the VTM. However, in the case of inter-predicted slices, the partition trees of Luma are utilized for the Chroma components.

### B. Transform Module

The concept of MTS in VVC introduces three distinct trigonometric transform types, which are Discrete Cosine Transform (DCT)-II/VIII and Discrete Sine Transform (DST)-VII. In the context of MTS, as depicted in Fig. 3, these

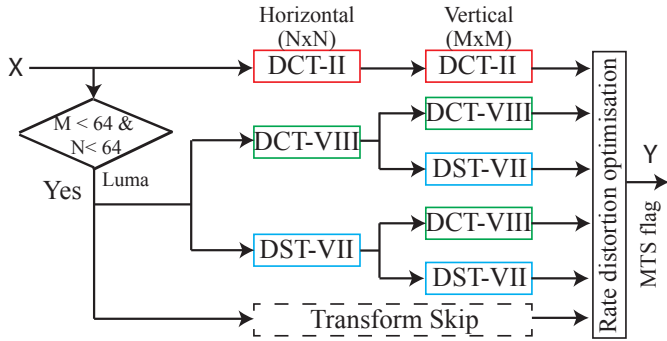


Fig. 3: The concept of 2D separable transforms selection in VVC.  $X$  is the input block of residuals,  $Y$  is the output transformed block and MTS flag is the index of the selected set of transforms.

transforms are chosen for Luma blocks smaller than 64, with the selection based on minimizing the rate distortion cost among five different transform sets and the skip configuration. However, for chroma components and Luma blocks of size 64, only DCT-II is considered. This utilization of the MTS solution results in a significant coding improvement, with gains of approximately 0.84% in All Intra (AI) and 0.33% in Random Access (RA) coding configurations when compared to HEVC [16].

The *sp\_s\_mts\_enabled\_flag*, which is defined in the Sequence Parameter Set (SPS), serves to enable the activation of the MTS concept within the encoder. In addition to this flag, two other flags are defined at the SPS level, one to signal the use of implicit MTS signaling for Intra-coded blocks and another to indicate the use of explicit MTS signaling for Inter-coded blocks. In the case of explicit signaling, which is the default mode in the Common Test Conditions (CTC), the *tu\_mts\_idx* syntax element is employed to convey information about the selected horizontal and vertical transforms. Finally, this flag is encoded using a Truncated Rice code with a rice parameter  $p = 0$  and  $cMax = 4$  (TRp).

The Low-Frequency Non-Separable Transform (LFNST) has been incorporated into VTM-5. This technique leverages matrix multiplication to process coefficients from the forward primary transform at the encoder side:

$$\vec{Y} = T \cdot \vec{X}, \quad (1)$$

where the vector  $\vec{X}$  includes the low frequency coefficients of the block rearranged in a vector and the matrix  $T$  contains the coefficients transform kernel. The LFNST is enabled only when DCT-II is used as a primary transform.

Four sets of two LFNST kernels of sizes  $16 \times 16$  and  $64 \times 64$  are applied on 16 coefficients of small block (min (width, height)  $< 8$ ) and 64 coefficients of larger (min (width, height)  $> 4$ ) blocks, respectively. The VVC specification defines four different transform sets selected depending on the Intra prediction mode and each set defines two transform kernels. The used kernel within a set is signaled in the bitstream. To reduce the complexity in number of operations and memory required to store the transform coefficients, the  $64 \times 64$  inverse transform is reduced to  $48 \times 16$ . Therefore, only 16 basis of the

transform kernel is used and the number of input coefficients is reduced to 48 by excluding the bottom right  $4 \times 4$  block (i.e., include only coefficients of the top-left, top-right and bottom-left  $4 \times 4$  blocks).

### C. Intra and Inter Prediction Tools

In VVC, there are 65 intra directional prediction modes compared to 33 in HEVC, capturing natural video's diverse edge directions. It employs rectangular blocks instead of just square ones in HEVC. Intra prediction modes are coded with a 6 Most Probable Modes (MPMs) list, unlike HEVC's 3 MPMs list. The VTM refines the planar mode's Intra prediction results using the Position Dependent Intra Prediction Combination (PDPC) method, a combination of unfiltered and HEVC-style intra prediction with filtered boundary samples. Additionally, VVC introduces Multiple Reference Line (MRL) intra prediction, using MRL instead of HEVC's nearest reference line, with the index signaled in the bitstream.

In the realm of Inter prediction, VVC incorporates a range of novel and improved coding tools, such as Subblock-based Temporal Motion Vector Prediction (SbTMVP), the Affine Motion Model (AFF), Bi-Directional Optical Flow (BDOF), and advanced Motion Vector (MV) prediction that inherits more information from reference, combine temporal and spatial prediction [14]. Additionally, the Decoder-side Motion Vector Refinement (DMVR) feature, present in VTM, optimizes bit-rate reduction in Inter prediction by refining motion vectors at the decoder.

### D. Entropy Coding and In-Loop Filtering

In contrast to HEVC, where transform coefficients of a coding block are coded using non-overlapped Coefficient Groups (CGs), each containing the coefficients of a  $4 \times 4$  block, VTM employs various CGs ( $1 \times 16$ ,  $2 \times 8$ ,  $8 \times 2$ ,  $2 \times 4$ ,  $4 \times 2$ , and  $16 \times 1$ ). Furthermore, significant changes are introduced to the core of the Context Adaptive Binary Arithmetic Coding (CABAC) engine in VVC compared to its design in HEVC. While the CABAC engine in HEVC employs a table-based probability transition process among 64 distinct representative probability states, VVC adopts a decode decision model with a 2-state approach and variable probability updating window sizes [17].

In the realm of in-loop filtering, VVC introduces an Adaptive Loop Filter (ALF) alongside the traditional deblocking filter and Sample Adaptive Offset (SAO). For the luma component, it selects one of 25 filters for each  $4 \times 4$  block based primarily on local gradient direction and activity. Additionally, VVC employs two diamond filter shapes, a  $7 \times 7$  diamond shape for the luma component and a  $5 \times 5$  diamond shape for chroma components.

## III. VVC CODING PERFORMANCE: QUALITY ENHANCEMENTS

In order to evaluate the coding performance of VTM compared to HEVC HEVC Model (HM), we have performed two types of quality evaluations: objective measurements and subjective assessments. These two methods are described below.

TABLE I: Performance of the main tools included in the VTM-5.0 software [16].

Module	Tool description	BD-BR
Frame partitioning	Triangular partition mode	0.35%
	Chroma separate tree	0.14%
	Sub-block transform	0.41%
Transforms	Multiple Transform Selection	0.33%
	Low-frequency non-separable tran.	0.79%
Inter Prediction	Decoder-side Motion Vector Refinement	0.82%
	Subblock-based temp. merging cand.	0.43%
	Affine motion model	2.53%
	Merge with MVD	0.58%
	Bi-directional optical flow	0.78%
	Temporal motion vector predictor	1.19%
Intra Prediction	Multi-reference line prediction	0.20%
	Intra sub-partitioning	0.13%
	Matrix based intra prediction	0.27%
In-Loop Filt.	Adaptive Loop Filter	4.91%
Quantization	Dependent Quantization	1.71%

### A. Objective Quality Measurements

The main goal of an objective quality assessment metric is to produce the highest quality rating possible close to that provided, on average, by a set of observers during a campaign of subjective tests (see Section III-B). Several metrics of different categories are used: Mathematical approaches, weighting approaches and by modelling the Human Visual System (HVS).

1) *PSNR Metric*: The PSNR metric is a purely “signal” measure. Whatever the nature of the stimuli (image, video), PSNR is a pixel-to-pixel treatment regardless of the 2D aspect of the image or video. PSNR is based on the Mean Squared Error (MSE), to evaluate the error between a degraded image and its reference version. It is defined by (2).

$$MSE = \frac{1}{NM} \sum_{i=0}^{N-1} \sum_{j=0}^{M-1} (Im_r(i, j) - Im_e(i, j))^2, \quad (2)$$

where  $N$  and  $M$  are the horizontal and vertical dimensions of the image,  $Im_r$  is the reference image and  $Im_e$  is the image to be evaluated.

The PSNR of a signal of amplitude  $A$  is defined by (3). A PSNR value greater than 40 dB usually indicates that the image or video to be evaluated is of very good quality.

$$PSNR = 10 \log_{10} \left( \frac{A^2}{MSE} \right), \quad (3)$$

with  $A = 2^\gamma - 1$  and  $\gamma$  is the video bitdepth.

For video sequences, which ordinarily consist of three color components ( $Y$ ,  $U$ ,  $V$ ), we use generally a weighted PSNR ( $wPSNR$ ) version. The weighted PSNR is computed by weighting three components  $Y$ ,  $U$  and  $V$  as bellow

$$wPSNR = \frac{6PSNR_Y + PSNR_U + PSNR_V}{8}. \quad (4)$$

PSNR is the most used commonly objective metric in all digital domains. It is easy and fast to implement. However,

it simply calculates the pixel-to-pixel resemblance without considering the relationships between these pixels.

2) *SSIM Metric*: To substantially remedy this disadvantage, Wang *et al.* [18] proposed a metric named Structural SIMilarity (SSIM) based on the similarities between the structures in the image. Thus, it makes it possible to extract three different criteria, for each “window” of the image, judged important for human observers, namely luminance, contrast and structure. It is given by:

$$SSIM(Im_r, Im_e) = \frac{(2\mu_{Im_r}\mu_{Im_e} + C_1)(2\sigma_{Im_r Im_e} + C_2)}{(\mu_{Im_r}^2 + \mu_{Im_e}^2 + C_1)(\sigma_{Im_r}^2 + \sigma_{Im_e}^2 + C_2)}, \quad (5)$$

where  $\mu_{Im_r}$  is the average neighborhood luminance,  $Im_r$ ,  $\sigma_{Im_r}$  is the standard deviation of the neighborhood,  $Im_r$ ,  $\sigma_{Im_r Im_e}$  is the covariance between  $Im_r$  and  $Im_e$ .  $C_1$  and  $C_2$  are two constants that depend on the dynamics of the image.

The values of this metric are then obtained for all calculation windows. They are between 0 and 1: a value close to 1 indicates that both images (videos) have a maximum fidelity while values close to 0 indicate a too degraded image (video). Moreover, SSIM has been recently exploited [19] in the HEVC rate-distortion optimization stage to enhance the perceived video quality under a rate control process.

3) *VMAF Metric*: Video Multi-Method Assessment Fusion (VMAF) is a perceptual video quality assessment algorithm developed by Netflix with collaboration of Laboratory of Image and Video Engineering (LIVE) [20]. VMAF is a full-reference, perceptual video quality metric focused on quality degradation due to compression and rescaling. It was specifically formulated to approximate human perception of video quality and then to correlate strongly with subjective Mean Opinion Score (MOS) scores. Using machine learning techniques, a large sample of MOS scores were used as ground truth to train a quality estimation model. VMAF estimates the perceived quality score by computing scores from multiple quality assessment algorithms and fusing them using a Support Vector Machines (SVM). VMAF has been shown to outperform other image and video quality metrics, such as SSIM and PSNR on several datasets in terms of prediction accuracy, when compared to subjective ratings.

4) *Bjontegaard Metric*: The Bjontegaard measure is become one of the most popular metric for video coding performance in the recent years. This metric is computed as a difference, in bit-rate, based on interpolating curves from the tested data points [21]. The comparison used the Bjontegaard-Delta bit-rate (BD-BR) measurement method, in which negative values tell how much lower the bit rate is reduced, and positive values tell how much the bit-rate is increased for the same PSNR quality [22].

### B. Subjective Quality Assessments

Unlike signal-based and HVS-based approaches for objective quality measurements, subjective quality assessment is the process of employing human viewers for grading video quality based on individual perception [3]. The global environment, viewing conditions and the implementation process

TABLE II: Configuration parameters for HM-16.20 and VTM main profiles, in RA configuration.

Parameter	HM-16.20 main	VTM-5.0 main
CTU size	64	128
QT max depth	4	4
MTT max depth	0	3
Transform Types	DCT-II, DST-VII	DCT-II, DST-VII, DCT-VIII
Max TU size	32	64
Loop Filters	DBF, SAO	DBF, SAO, ALF
Search Type	TZ	TZ
Search Range	384	384
N. Ref. Pictures	5	5
Entropy Coding	CABAC	CABAC
Internal Bit Depth	10	10

for subjective quality assessments are specified in various ITU recommendations. Two specific methodologies are widely used in the video quality assessments: ITU-T Rec. P.910 [23] for multimedia applications and ITU-R Rec. BT.500 [24], for television pictures.

1) *Experimental environment*: The subjective study has been conducted in the INSA/IETR PAVIM Lab, which is a platform for video quality monitoring actively involved in the emerging video contents. This platform includes a psychovisual testing room, complying with the ITU-R BT.500-13 Recommendation. A display screen Ultra High Definition (4K) of 55 inches Loewe Bild 7.55 was used to visualise the video sequences. 44 observers, 30 men and 14 women aged from 20 to 55 years, have participated in this experiment. All the subjects were screened for color blindness and visual acuity using Ishihara and Snellen charts, respectively, and have a visual acuity of 10/10 in both eyes with or without correction. Finally, all participants have been gratified. Viewers are placed at distances of 1.5 and 3 times the height of the screen for UHD and HD resolutions, respectively. In this section, we provide information regarding the used video sequences, test material, test settings, and evaluation procedures.

2) *Test Video Sequences*: In this experiment, a set of high resolution video sequences, from various categories (music, sport, gaming, etc.) has been selected from several datasets (Huawei, SVT, b<>com) as well as 4EVER<sup>1</sup> database. The target resolutions for this test are HD (i.e. 1920×1080) and UHD (3840×2160), in a Standard Dynamic Range (SDR). Firstly, 13 videos sequences in UHD (4K) resolution have been selected and down-sampled using the Scalable SHVC down sampling filters. The choice of these video is mainly based on the video encoding complexity in terms of colour, movement, texture and homogeneous content.

All these videos were encoded using both HEVC (HM-16.20) and VVC (VTM) main profiles, at different bit-rates, in HD and UHD format in RA configurations. The main profiles configuration parameters are summarized in TABLE II. This first selection is done in order to retain the sequences representing a good balance of content variety and video coding artifacts. After this initial selection, only seven scenes have been retained for the experiment, as given in Table III.

<sup>1</sup>For Enhanced Video ExpeRience 2 project, www.4ever-2.com

TABLE III: Test video sequences

Sequence	HD	UHD	Fps	Bit Depth
<i>AerialCrowd2</i>	1920 × 1080	3840 × 2160	30	10
<i>CatRobot1</i>	1920 × 1080	3840 × 2160	60	10
<i>CrowdRun</i>	1920 × 1080	3840 × 2160	50	8
<i>DaylightRoad</i>	1920 × 1080	3840 × 2160	60	10
<i>Drums2</i>	1920 × 1080	3840 × 2160	50	10
<i>HorseJumping</i>	1920 × 1080	3840 × 2160	50	10
<i>Sedof</i>	1920 × 1080	3840 × 2160	60	8

In total 168 video sequences are used in this study: 7 scenes × 5 bit-rates × 2 codecs × 2 resolutions + 28 original scenes (2 references per scene in two resolution).

In order to measure video contents diversity across the selected test sequences, Spatial Information (SI) and Temporal Information (TI) metrics are used [25]. The SI estimates the amount of spatial details whereas the TI measures the quantity of motion in the sequence. In Fig. 4, the 14 test sequences are represented under the SI TI coordinates. The green crosses and red stars correspond to UHD (4K) and HD test sequences, respectively. Fig. 4 shows that the down-sampled HD sequences have equivalent TI coordinates and significantly higher SI coordinates compared to the original UHD sequences. This is due to the increased quantity of spatial details contained in the down-sampled HD frames compared to the original UHD (4K) frames, since the same visual information is located in a smaller frame.

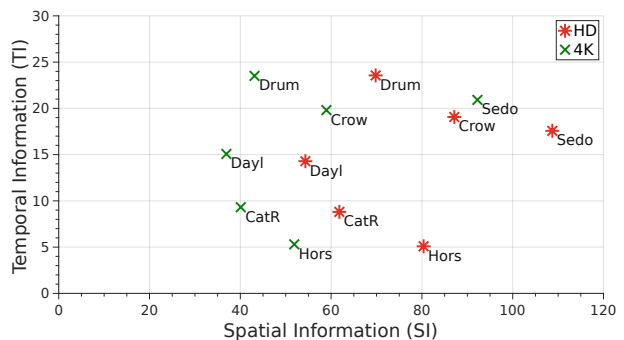


Fig. 4: SI and TI of the test sequences, according to the resolution.

3) *Evaluation Procedure*: In this quality assessment experiment, the Subjective Assessment Methodology for Video Quality (SAMVIQ) method was used [26]. This method has specifically been designed for multimedia content. It takes into account a range of codec types, image formats, bit-rates, temporal resolutions, etc. It has been recommended by ITU-R 6Q in 2004 [27]. Each scene (video sequence) is presented with the following conditions: an explicit reference, a hidden reference and 10 Processed Video Sequences (PVSs). Four categories of PVS are tested (HEVC-HD, VVC-HD, HEVC-UHD and VVC-UHD). The button with label REF clearly identifies the explicit reference sequence. The hidden reference is identical to the explicit reference but it is not readily accessible to the subject and it is "hidden" among other stimuli. For each scene, participants were asked to evaluate

the processed video sequences, given by buttons with letter labels A to K (including the hidden reference), as indicated by the protocol SAMVIQ [28]. The conducted experiment is divided into two parts: HD and UHD. For an optimal visual comfort, these two parts have been done separately but using the same participants. Moreover, to prevent from visual fatigue, each part (HD and UHD) of the test is carried-out in two sessions. Before each experiment, participants receive clear and deep explanations about the evaluation procedures and the used interface. Finally, all viewers scores have been collected using a dedicated Graphical User Interface (GUI), developed in compliance with the SAMVIQ recommendation.

#### IV. QUALITY EVALUATION RESULTS

##### A. Objective Evaluation Results

The analysis given here is based on the four objective metrics described above: PSNR, SSIM, VMAF and Bjøntegaard Measure (BD-BR). The objective quality results, for the whole test sequences, are shown in Fig. 5 in the form of PSNR (top), SSIM (middle) and VMAF (bottom) versus bit-rate plots. The solid and dotted lines represent HEVC and VVC codec curves, respectively. It is worth noting here that the objective (i.e., PSNR, SSIM, VMAF) and subjective (i.e., MOS) results are independently analyzed, and thus no direct correlation between them is demonstrated, since we do not develop here a new objective quality metric. Also, the PSNR results presented here are weighted through the three components ( $y$ ,  $u$ ,  $v$ ), as shown in the Equation (4). Figs. 5 (top) illustrates the average performance in terms of PSNR metric of the whole used dataset. According to these figures, PSNR values increase significantly when using VTM coding tools, and consequently VTM enables higher video quality than the HM codec. In addition, it can be observed that VVC codec achieves the same objective quality as HEVC while typically requiring substantially lower bit-rates. In these figures, VVC codecs enable a bit-rate saving up to 40% for some sequences as *CatRobot* and *DaylightRoad* in the two used formats HD (left) and UHD (right).

The obtained results using SSIM metric, Figs. 5 (middle), have shown also that VVC codecs enables a bit-rate saving up to 50% for some test sequences, in HD (left) and UHD (right) formats, compared to the HEVC standard. In these figures, we can noticed that except for the *CrowdRun* sequence in low bit-rate, all the used test sequences have a good quality measures: higher than 0.96 in HD and 0.97 in UHD (4K) formats. For some sequences, as *AerialCrowd2* in HD and *DaylightRoad* in UHD formats, a considerable bit-rate gains is obtained by VVC codec while keeping the same quality measures. In other words, for the same quality at high bit-rate ( $> 0.99$ ), a bit-rate gain from 6Mbps to 8Mbps is obtained. This gain is ranking from 13Mbps to 21Mbps in UHD (4K) format.

Finally, Figs. 5 (bottom) present the objective measurements using VMAF metric, in HD (left) and UHD (right) contents. Similar to the other metrics, these figures indicate that VVC codecs enable a bit-rate saving up to 49% compared to HEVC standard. It is noticed here that we have used these metrics, while presenting the similar behaviours, in order to cover a

large number of quality measurement categories, for a possible future comparisons as well as a multiple ground truth datasets.

Table IV summarizes the Bjøntegaard measurement (BD-BR) for HD and UHD contents, using PSNR metric. On average, the VTM codec enables, in average, a bit-rate savings of about 31% and 34% for HD and UHD (4K) video sequences, respectively. Moreover, using VMAF and SSIM, the same behaviors are noticed and a significant bit-rate gains is obtained. These gains are summarized in Table VI.

TABLE IV: BD-BR (PSNR) of VTM-5 compared to the anchor HM video codec.

Sequence	BD-BR (HD)	BD-BR (UHD)
<i>AerialCrowd2</i>	-24,5%	-29,9%
<i>CatRobot1</i>	-39,8%	-41,8%
<i>CrowdRun</i>	-27,2%	-30,3%
<i>DaylightRoad</i>	-38,9%	-42,4%
<i>Drums2</i>	-29,5%	-32%
<i>HorseJumping</i>	-31,1%	-32,5%
<i>Sedof</i>	-27,7%	-31,9%
<b>Average</b>	<b>-31.24%</b>	<b>-34.42%</b>

##### B. Subjective Assessment Results

The first step in the results analysis is to calculate the Mean Opinion Score (MOS) for each video used in the experiment. This average is given by the equation 6.

$$MOS_{jk} = \frac{1}{N} \sum_{i=1}^N s_{ijk}, \quad (6)$$

where  $s_{ijk}$  is the score of participant  $i$  for the test video  $j$  of the sequence  $k$  and  $N$  is the number of observers. In order to better evaluate the reliability of the obtained results, it is advisable to associate for each MOS score a confidence interval, usually at 95%. This is given by the equation 7. Scores respecting the experiment conditions must be contained in the interval  $[MOS_{jk} - IC_{jk}, MOS_{jk} + IC_{jk}]$ .

$$IC_{jk} = 1.95 \frac{\delta_{jk}}{\sqrt{N}}, \quad \delta_{jk} = \sqrt{\frac{\sum_{i=1}^N (s_{ijk} - MOS_{jk})^2}{N}}. \quad (7)$$

Before data analysis, we conducted a verification of the distribution of individual participant scores. In fact, some data may parasite the results. Thus, a filtering procedure was applied to obtained results based on the annex 2 of the ITU-R BT.500 recommendation [27]. In our outlier detection verification, a correlation index greater (Minimum between Pearson and Spearman correlations) than or equal to 0.75 is considered as valid for the acceptance of the viewer's scores; otherwise, the viewer is considered as an outlier. Following this screening process, 8 subjects (6 in HD and 2 in UHD test) were discarded. Consequently, only 36 viewers scores are retained.

Table V summarises the BD-Rate gains obtained by VVC relative to HEVC, considering MOS. As shown in this table, VTM outperforms the HEVC for the whole used sequences.

A bit-rate savings of about 37% and 40% are obtained for HD and UHD (4K) video sequences, respectively

The subjective evaluation results, for the whole test sequences are shown in Figs. 6 & 7 in the form of MOS versus bit-rate plots, for HD and UHD (4K) formats, respectively. The solid and dotted lines represent HEVC and VVC codec curves, respectively. The associated confidence intervals are displayed for each MOS test point. In these figures, VTM codec enables a higher MOS score and consequently a higher video quality, compared to HEVC reference software. As we can see, a considerable gains in terms of bit-rate savings can be noticed with the same perceived quality. For HD format , a bit-rate saving of -50% and -40% is obtained in the “Excellent” and “Good” quality area, respectively. For UHD format, a bite-rate savings of about -50% is obtained, with the same perceived quality, for the sequence *CatRobot1*. Reciprocally, for the same bit-rate, a considerable quality enhancement is obtained by VVC compared to HEVC standard. In fact, at low bit-rate, the sequence “CrowdRun” is judged as “Fair” quality using VVC while it is judged as “Poor” quality using HEVC standard. In addition, this quality is enhanced from “Fair” to “Good” quality area using VVC. The same behavior can be noticed for the other video sequences, depending on the considered bit-rates and the used video format.

TABLE V: BD-BR (MOS) of VTM compared to the anchor HM-16.20 video codec.

Sequence	BD-BR (HD)	BD-BR (UHD)
<i>AerialCrowd2</i>	-33%	-41%
<i>CatRobot1</i>	-48%	-47%
<i>CrowdRun</i>	-35%	-35%
<i>DaylightRoad</i>	-49%	-48%
<i>Drums2</i>	-35%	-39%
<i>HorseJumping</i>	-38%	-45%
<i>Sedof</i>	-19%	-21%
<b>Average</b>	<b>-37%</b>	<b>-40%</b>

As a conclusion, for HD resolution, a bit-rate saving of 31% and 35% can be achieved with the VTM in terms of PSNR and VMAF metrics, respectively. This gain exceeds 40% for the UHD resolution, using VMAF metric. For the subjective comparison, the obtained gains is ranging between 37% and 40% for HD and UHD resolutions, respectively, as summarized in Table VI. For the same bit-rate range, the highest bit-rate saving for HD contents is obtained by MOS-based BD-rate (-37%) while this gains for UHD contents is obtained by VMAF-based BD-rate (-40.44%).

### C. Statistical Analysis

A statistical analysis was performed using the Analyse of Variance (ANOVA) approach [29]. Bit-rate, Content, Resolution and Codec are used as independent variables and MOS is used as dependent variable. The null hypothesis in this case would be that theVVC test points have the same quality as the HEVC test point while the alternate hypothesis is that the VVC test points do not have the same perceived quality as the HEVC test point [29]. Results have shown that only codec parameter (VTM, HM) has a significant influence on the subjects scores,

with  $p\text{-value} < 0.0001$ <sup>2</sup>. Subjectively speaking, VVC standard enables a significant visual quality improvement regardless the used bit-rate, resolution and video content.

TABLE VI: Bit-rate Savings of VTM over HEVC standard.

Resolution	PSNR	VMAF	SSIM	MOS
HD	-31.24 %	-35.18 %	-33%	<b>-37%</b>
UHD	-34.42%	<b>-40.44%</b>	-38%	-40%

## V. VVC CODING TIME AND COMPLEXITY REPARTITION

This section provides an analysis of times and complexity repartitions, for both encoding and decoding processes. In order to highlight the principal evolutions from one reference software to another, the VTM and HM results are presented simultaneously.

### A. Platform and Configuration Parameters

The experiments are carried-out on the same 14 sequences described in Section III-B2. In order to evaluate the impact of Quantization Parameter (QP) on encoding and decoding times, 2 QP values per resolution are selected. Encodings of HD sequences with QP=37 generate bit-rates considered too small to be representative of real use-cases, and bit-rates generated by UHD sequences encodings with QP=27 are considered too large. For this reason, the aforementioned QP values are discarded in the following experiments. Finally, four QP values are retained in the following experiments: QP=27 and QP=32, for HD sequences, and QP=32 and QP=37, for UHD (4K) sequences.

TABLE VII: Platform setup for complexity analysis

<b>Central Processing Unit (CPU)</b>	Intel Xeon CPU E5-2603 v4
<b>Clock Rate</b>	1.70 GHz
<b>Memory</b>	8 Gb
<b>Compiler</b>	gcc 5.4.0
<b>Operating System</b>	Linux 4.4.0-127-generic

TABLE VII details the platform setup for complexity analysis. The experiments on codecs time and complexity repartition are carried-out on an Intel(R) Xeon(R) CPU E5-2603 v4, a CPU clocked at 1.70 GHz. The HM and VTM are both built with gcc compiler version 5.4.0, under Linux version 4.4.0-127-generic as distributed in Ubuntu-16.04.

By default, the VTM features low-level optimizations, such as Single Instruction on Multiple Data (SIMD) optimizations, at both encoder and decoder sides. SIMD describes computers that perform the same operation on multiple data simultaneously, with a single instruction. To assess the time consumption of the VTM without low-level optimizations, the SIMD optimizations at both encoder and decoder sides are disabled in the following. This also enables a fair comparison with the HM software that does not include any SIMD optimisation. The speed-up offered by SIMD optimizations is nonetheless measured and further discussed.

The repartition of encoding and decoding complexities, presented in upcoming Sections V-B2 and V-C2, are obtained

<sup>2</sup>a factor is considered influencing if  $p\text{-value} < 0.05$

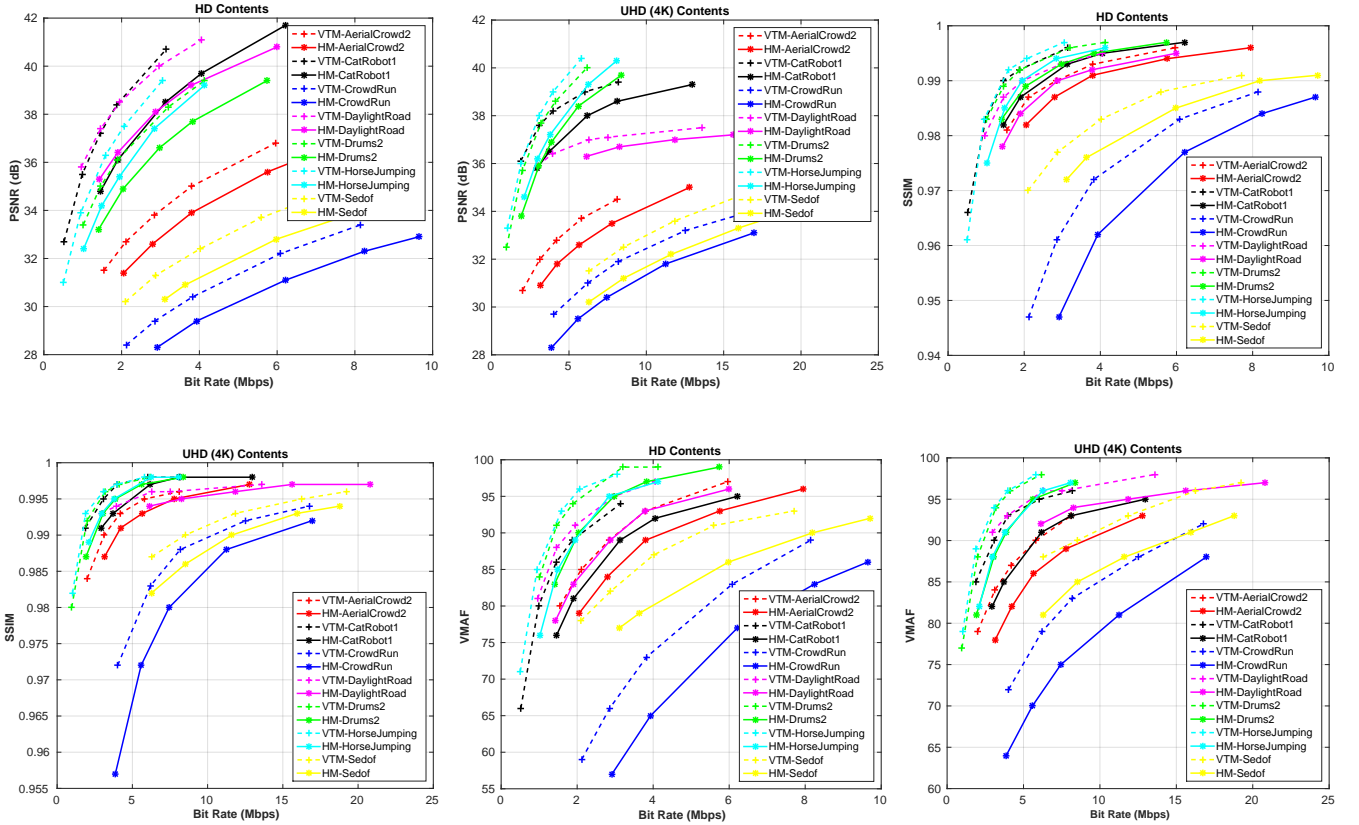


Fig. 5: Objective-based comparison, using three metrics: PSNR (top), SSIM (middle) and VMAF (bottom), for the whole used datasets in HD and UHD (2160p) formats.

by running the executables with Callgrind [30]. Callgrind is the Valgrind profiling tool that records the call history of program functions as a call graph. By default, the data collected includes the number of instructions executed, the calling/callee relation between functions and the number of calls. Contrary to execution time, that depends among others on memory accesses or CPU frequency, the insight of the complexity repartition given by Callgrind is nearly constant regardless of the execution platform.

## B. Encoders Analysis

### 1) Encoding Time:

TABLE VIII shows an average factor of 1,700 between real-time encoding and the HM encoding time of HD video content at QP=32. This average factor is 16 time greater (27,000) with VTM. The VTM main profile is therefore 16 times more complex in average compared to the HM main profile for the encoding of HD video content. This encoding complexity increase between HM-16.20 and VTM-5.0 is mainly caused by the the additional transform types and intra modes enabled in VTM-5.0, and by the MTT partitioning which allows 4 additional partition modes compared to QT partitioning in HM.

The results in TABLE VIII also highlight the impact of QP value on encoding complexity. Indeed, in order to avoid exhaustive Rate Distorsion Optimization (RDO) process and to decrease encoding time for researchers experimentations, the reference encoders include early termination techniques.

TABLE VIII: Factor between encoding time and real time (x1000), for both VTM-5.0 and HM-16.20 in RA configuration, according to the test sequence and QP value.

Encoder	HD		UHD					
	HM-16.20	VTM-5.0	HM-16.20	VTM-5.0	HM-16.20	VTM-5.0		
QP	27	32	27	32	32	37	32	37
<i>AerialCrowd2</i>	1.1	0.9	22	15	3.9	3.4	64	41
<i>CatRobot1</i>	2.0	1.8	33	26	7.2	6.7	102	68
<i>CrowdRun</i>	2.4	2.1	49	39	8.6	7.6	179	124
<i>DaylightRoad</i>	2.3	2.0	44	32	8.1	7.3	132	84
<i>Drums2</i>	2.1	1.9	42	32	7.4	6.7	107	72
<i>HorseJumping</i>	1.4	1.3	23	17	5.4	5.0	57	38
<i>Sedof</i>	2.2	1.9	40	28	7.9	7.1	129	85
<b>Mean</b>	<b>1.9</b>	<b>1.7</b>	<b>36.2</b>	<b>26.9</b>	<b>6.9</b>	<b>6.3</b>	<b>110.3</b>	<b>73.2</b>
<b>Std Dev</b>	<b>0.4</b>	<b>0.4</b>	<b>9.8</b>	<b>7.9</b>	<b>1.5</b>	<b>1.4</b>	<b>38.9</b>	<b>27.3</b>

In VTM for instance, a dozen early termination techniques speed-up the encoding process by a factor 8 [31] compared to exhaustive RDO process. The efficiency of these techniques vary with the encoding parameters, in particular with QP value. This explains why in TABLE VIII, for VTM, encoding times carried out with lower QP values are 44% higher compared to encodings with higher QP values. The impact of QP decreases to 11% for HM, due to QT partitioning that offers less early termination opportunities compared to MTT partitioning in VTM.

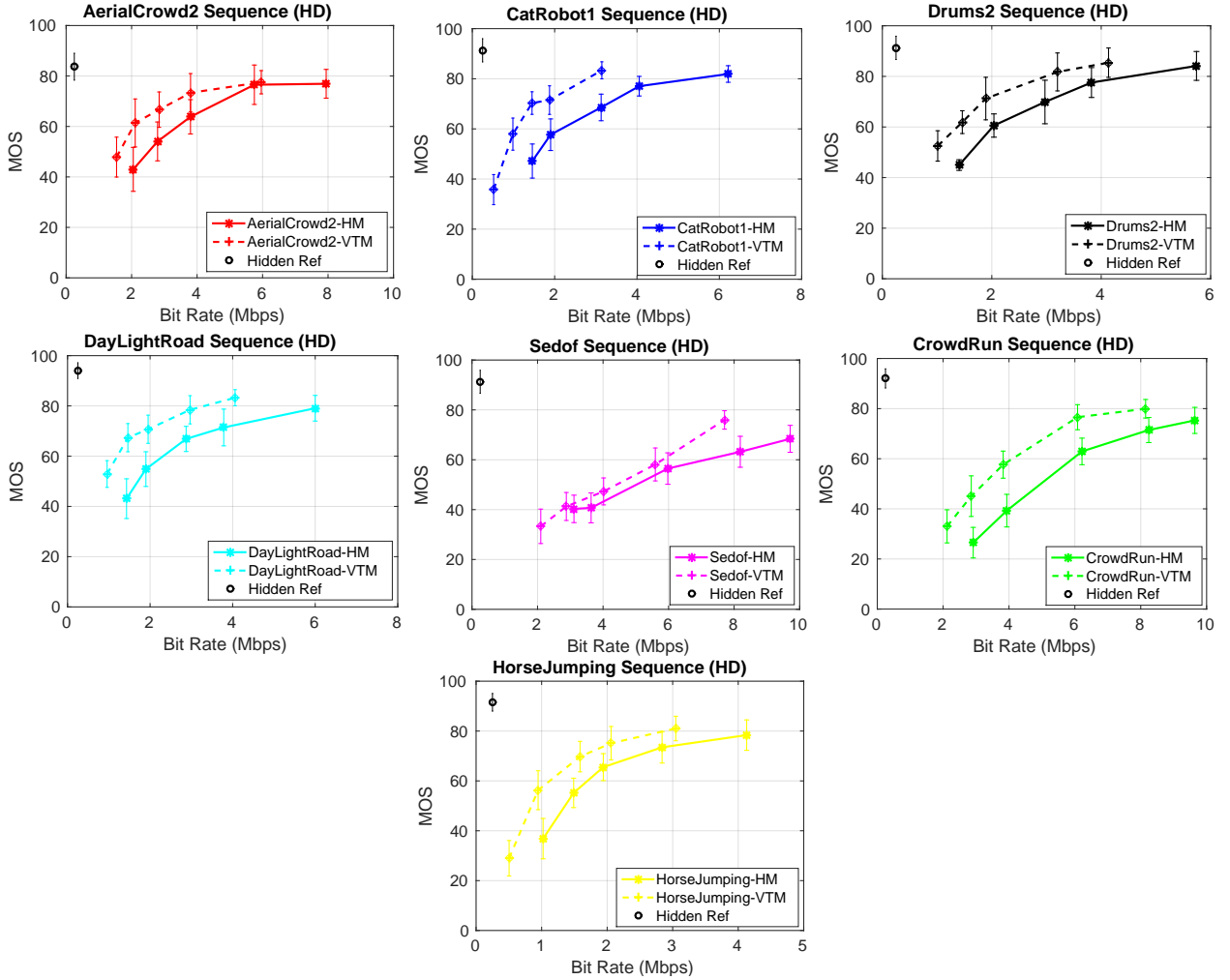


Fig. 6: MOS-based comparison, with associated 95% confidence intervals, in HD format.

Regardless the QP value and resolution, encoding times standard deviations are around 20% and 30% of average encoding times for HM and VTM, respectively. These standard deviations are induced among others by the diversity of frame-rates among test sequences. For instance, the sequence *AerialCrowd2* with the lowest frame-rate (30 frames/sec) has the lowest encoding time in all columns of TABLE VIII. The standard deviations are also a consequence of the diversity of spatial textures and movements among test sequences. Let us consider the sequences *HorseJumping* and *CrowdRun*, which have the same frame-rate of 50 frames/sec. Fig. 4 shows that *CrowdRun* has considerably higher SI and TI compared to *HorseJumping*. Given that previously mentioned early termination techniques are more efficient on sequences with lower spatial textures and slower motion, *CrowdRun* encoding time exceeds at least by a factor 1.4 *HorseJumping* encoding time, in all columns of TABLE VIII.

As mentioned in Section V-A, SIMD optimizations have been disabled in the VTM encoder in this work. Enabling the SIMD optimizations speeds up the VTM encoder by 1.9 times in average. This speed-up is very far from the 110,000 speed-up needed in average to achieve UHD real time encoding. Complexity reduction of HEVC encoder has

been widely investigated [32], [33] in the past years, and recently more efforts have been dedicated to the VVC encoder. In fact, several techniques already proposed to reduce VTM encoding complexity by predicting a reduced set of likely intra modes [34], [35], or by testing a reduced number of partition configurations [36], [37]. We believe that the reduction of the VTM encoding complexity will be an active research field over the next years.

## 2) Encoding Complexity Repartition:

As mentioned in Section V-A, the encoding complexity repartition is obtained with Callgrind profiling tool. The encoders of both HM16.20 and VTM have a significant portion of its complexity located in code cycles, since functions call each other in a recursive manner during the partitioning. However, the graphical user interface for Callgrind data visualization, named KCachegrind, contains a cycle detection module that allows an easy profiling of encoding complexity.

Fig. 8 displays under the form of pie charts the encoding complexity repartition (in %), for UHD (4K) sequence *CrowdRun*, according to the reference software and QP value. The inter prediction stage is divided into 2 sub stages: Motion Estimation (ME) and Motion Compensation (MC). ME establishes the list of MV predictor candidates for the processed

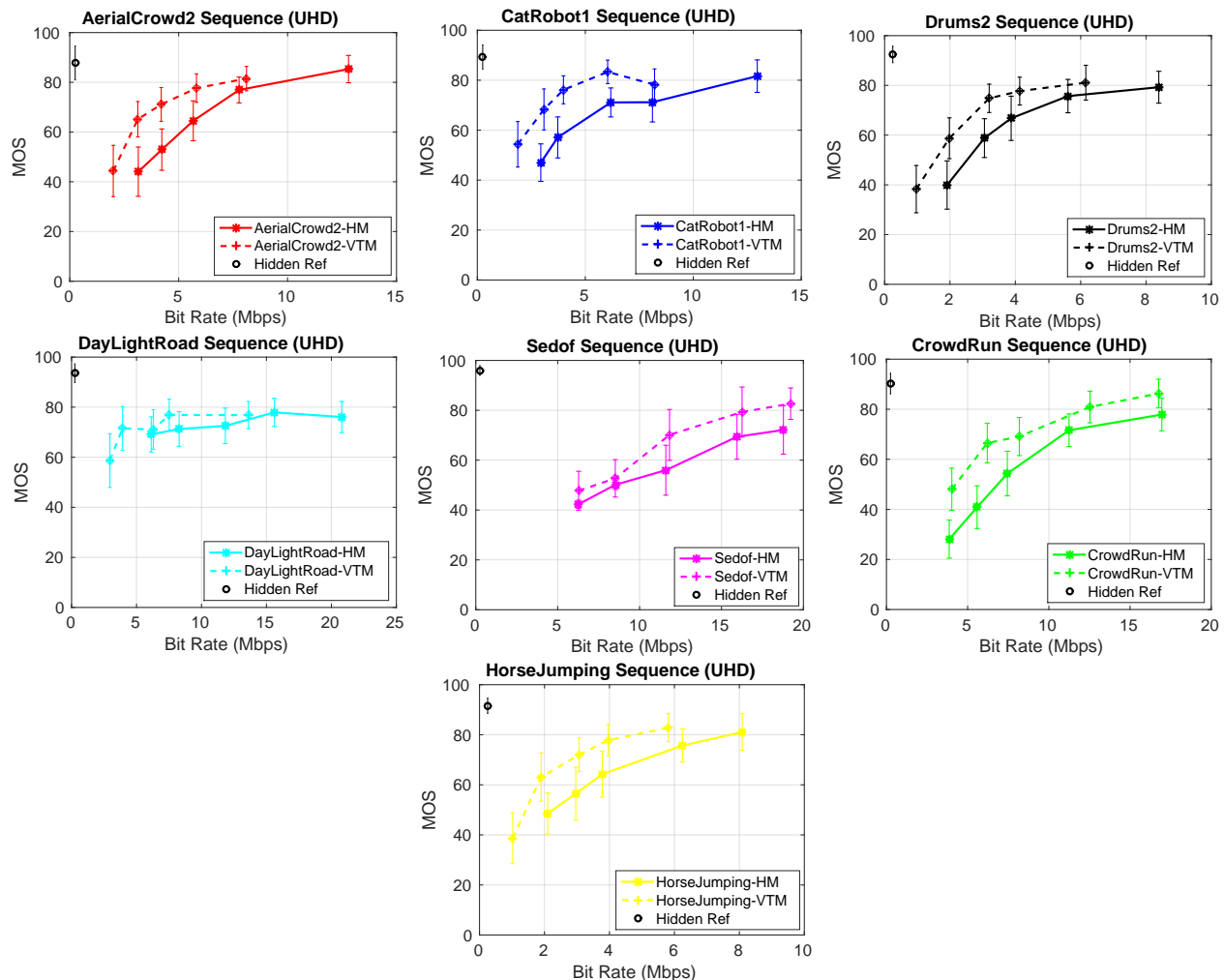


Fig. 7: MOS-based comparison, with associated 95% confidence intervals, UHD (4K) format.

CU and then infers the best MV predictor from this list. MC produces the prediction residuals by subtracting the inter predictions from the current original CUs. The  $Tr/Inv.Tr$  stage sums the complexities induced by both Transform and Inverse Transform stages. The stages representing less than 1% of encoding complexity are gathered in the “Other” category.

In RA configurations, Intra prediction and Inter prediction are in competition for Prediction Units (PUs) of P and B frames. As expected, Fig. 8 shows that Inter prediction is heavily predominant compared to Intra prediction for both HM and VTM. The percentage is even more unbalanced between Intra and Inter prediction when QP value increases. Indeed, Intra prediction percentage decreases from 3.4% and 18.8%, at QP=32, to 2.5% and 11.6%, at QP=37, while ME percentage raises from 55% and 41%, at QP=32, to 59% and 53%, at QP=37, for HM and VTM, respectively. Therefore Fig. 8 highlights that the higher the QP value, the more predominantly the encoder elects Inter prediction compared to Intra prediction.

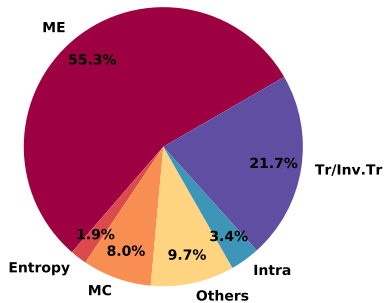
In Fig. 8, substantial differences are observable between HM and VTM complexity repartitions, especially for Intra Prediction and MC stages. The Intra Prediction percentage is

increased by almost a factor 5 in VTM compared to HM. This increase is caused by the Intra prediction tools added in VTM and mentioned in Section II, such as Multi-reference line prediction, Intra sub-partitioning and Matrix based intra prediction. The Bi-directional optical flow, DMVR and Affine motion model tools, also mentioned in Section II, have been introduced in the VTM and are applied during the MC stage. These new tools are responsible for 1.0%, 1.4% and 2.9% of total VTM complexity, respectively. Therefore they partly explain the increase in MC stage percentage in VTM (around 15%) compared to HM (around 8%). Finally, it is interesting to notice that the SAO and deblocking filters do not appear in Fig. 8 as their complexities are below 0.2% for both HM and VTM. However, ALF process must be taken into account in VTM, since its complexity represents 1.3% and 1.7% of total encoding complexity at QP=32 and QP=37, respectively.

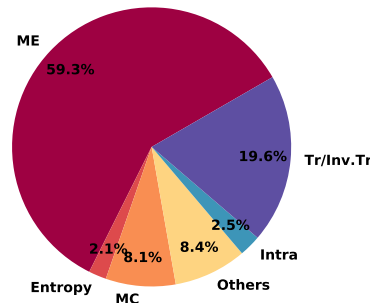
### C. Decoders Analysis

#### 1) Decoding Time:

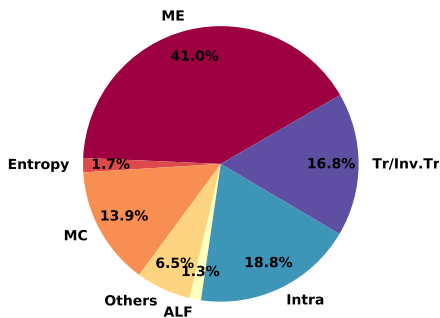
The decoding process interprets the encoded symbols of a bitstream compliant with the standard specification. It is therefore not burdened with the complex RDO performed



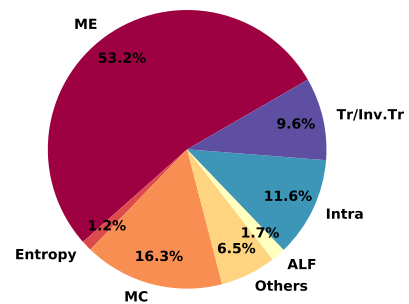
(a) HM-16.20, QP=32 (8.6 Ks)



(b) HM-16.20, QP=37 (7.6 Ks)



(c) VTM-5.0, QP=32 (179 Ks)



(d) VTM-5.0, QP=37 (124 Ks)

Fig. 8: Encoding complexity repartition (in %), for UHD sequence CrowdRun, according to the reference software and QP value.

TABLE IX: Factor between decoding time and real time, for both VTM-5.0 and HM-16.20 in RA configuration, according to the test sequence and QP value.

Decoder	HD				UHD			
	HM-16.20		VTM-5.0		HM-16.20		VTM-5.0	
QP	27	32	27	32	32	37	32	37
<i>AerialCrowd2</i>	2.8	2.3	8.8	7.8	8.4	7.3	27.9	25.7
<i>CatRobot1</i>	4.1	3.6	13.1	11.1	13.1	12.1	44.4	35.5
<i>CrowdRun</i>	5.4	4.4	15.4	13.1	14.2	12.1	49.0	39.6
<i>DaylightRoad</i>	4.5	4.0	15.1	13.8	13.5	12.6	54.2	42.3
<i>Drums2</i>	4.3	3.7	12.1	10.8	12.0	11.3	37.1	31.0
<i>HorseJumping</i>	3.1	2.7	10.8	8.0	10.8	10.0	32.5	28.4
<i>Sedof</i>	4.9	4.1	15.7	14.7	13.9	12.2	52.9	50.7
<b>Mean</b>	<b>4.1</b>	<b>3.5</b>	<b>13.0</b>	<b>11.3</b>	<b>12.3</b>	<b>11.1</b>	<b>41.4</b>	<b>36.1</b>
<b>Std Dev</b>	<b>0.9</b>	<b>0.7</b>	<b>2.5</b>	<b>2.4</b>	<b>1.9</b>	<b>1.7</b>	<b>8.4</b>	<b>8.0</b>

during encoding process that includes among others partitioning, intra mode decision or motion estimation. For this reason, comparatively to encoding time values presented in TABLE VIII, the decoding times shown in TABLE IX are in average 500 and 2000 times lower compared to encoding times for HM and VTM-5.0, respectively.

It is interesting to note that the decoding time with VTM is almost 3 times greater compared to the decoding time with

HM. This decoding complexity increase is partly imputable to the ALF filter introduced in VTM, which complexity will be further discussed in Section V-C2. Moreover, regardless of the resolution or test sequence, the decoding time decreases with the QP value in TABLE IX for both HM-16.20 and VTM-5.0. Indeed, for a given sequence, a lower QP value implies a larger bitstream outputted by the encoder, and therefore more symbols for the decoder to interpret especially at the level of the CABAC engine.

As mentioned in Section V-A, SIMD optimizations have been disabled at VTM decoder side. Enabling the SIMD optimizations speeds up the VTM decoder by 2.0 times in average for both HD and UHD sequences. Therefore, by enabling SIMD optimizations, the VTM decoding time is only 1.5 times greater than HM in average. For HEVC standard, real-time decoding has been reached by adding hardware optimization, implementing assembly written functions and/or enabling high level parallelism. For instance, authors in [38] describe a real-time SHVC decoder based on the OpenHEVC open source decoder, and paper [39] presents a real-time decoder for HEVC standard relying on SIMD optimizations and frame-level parallelism. In order to achieve real-time decoding for VVC standard, similar efforts must be extended and improved in future years, since we have shown that decoding process is 3 times more complex for VVC standard compared to HEVC

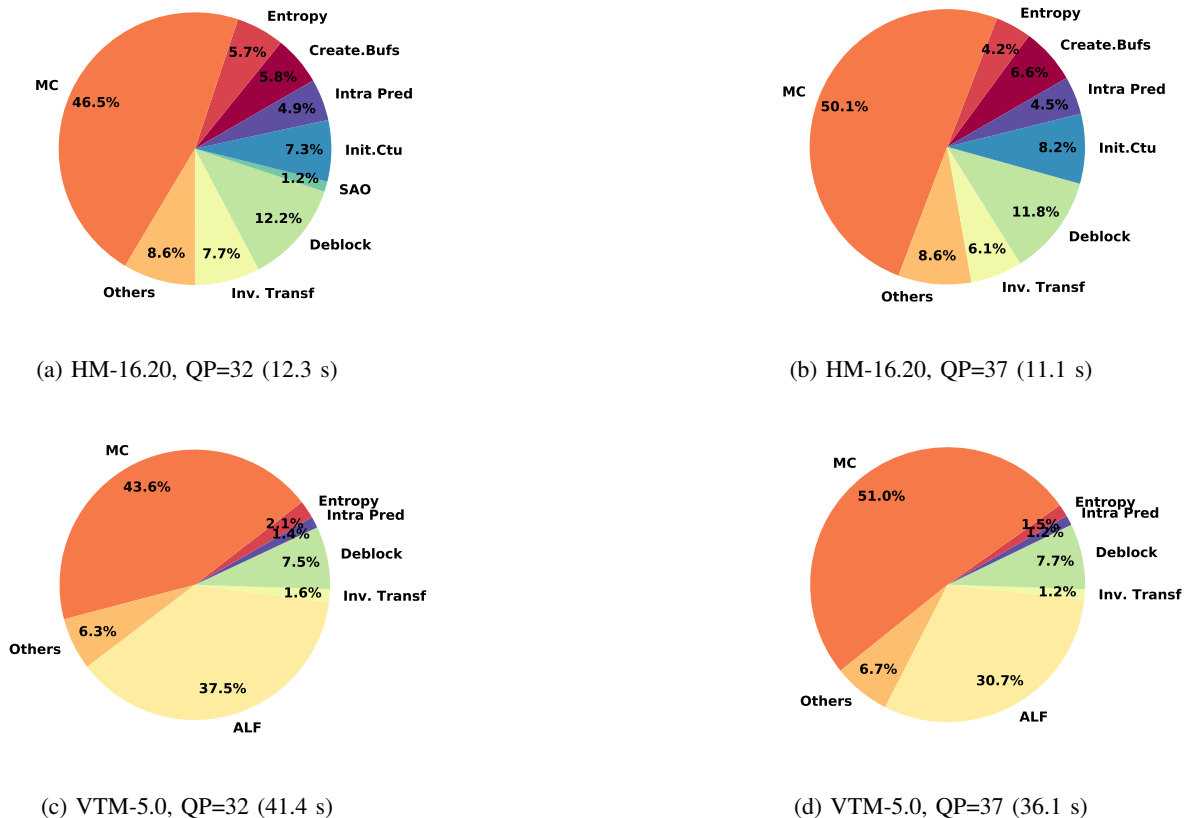


Fig. 9: Decoding complexity repartition (in %), averaged across UHD test sequences, according to the reference software and QP value.

standard.

### 2) Decoding Complexity Repartition:

As for the encoder in Section V-B2, the decoding complexity repartition is obtained by running the decoder with Callgrind [30]. Fig. 9 displays the decoding complexity sharing (in %), averaged across UHD test sequences, according to the reference software and QP value. The Create Bufs. stage consists in the creation of global buffers at picture level, while Init CtU creates internal buffers and sets initial values before encoding the CTU. The sum of these stages is greater than 13% in HM, but is negligible in VTM.

The first noticeable fact among the presented pie charts is the predominance of MC, ranging from 43.6% to 51.0% in both HM and VTM. The predominance of Inter predicted frames in RA configuration explains these numbers, and also explains the limited portion of Intra prediction in the pie charts. In VTM, an important share of MC complexity lies in the DMVR, that refines the motion vectors at decoder side, as mentioned in Section II. In fact, the share of DMVR in VTM global decoding complexity is in average 23% with QP=32 and 32% with QP=37, which represents almost 60% of MC stage complexity. However, the DMVR is not significant burden as the previous percentages suggest for the decoding process. Indeed, when it is disabled, it is replaced to a large extent by usual MV Inter prediction, which decoding complexity approaches DMVR complexity. The contribution [16] confirms

this behaviour, since it announces that VTM decoding complexity is only 4% lower when DMVR is disabled compared to original VTM in RA configurations. The deblocking filtering stage covers a consistent portion of the total decoding complexity: around 7.5% for VTM and around 12% for HM. In VTM, the in-loop filtering percentage is heavily increased by additional ALF tool, which is responsible for around a third of total decoding complexity. As mentioned in Section II, the ALF provides a significant improvement in encoding efficiency. It does not overload the VTM encoding process by more than 2% of total complexity (see Fig. 8). However, in counterpart for the aforementioned benefits, ALF represents a considerable burden for the decoding process. It is worth mentioning that ALF percentage decreases to less than 20% when the SIMD optimizations are enabled.

## VI. CONCLUSION

In this paper, we have conducted a comprehensive investigation into the quality assessments and the associated computational complexities of the VVC standard in comparison to the HEVC reference software. Our study focused on examining the bit-rate savings achieved between VTM and the HM software, as well as the distribution of encoding/decoding complexities across a typical classification of hybrid decoding tools. Our findings reveal that VTM's coding tools consistently deliver a substantial improvement in video quality compared

to the HM reference software across various video sequences used in our experiments. Utilizing quality metrics such as PSNR, SSIM, and VMAF, we observed gains ranging from 31% to 40%, with the specific value depending on the chosen quality metric. Subjectively, VTM significantly outperforms the HEVC reference software, particularly at lower bit-rates, achieving gains of up to 40%. Furthermore, our analysis indicates that, for various sequences, the VVC codec can provide equivalent perceived visual quality to HEVC while achieving bit-rate reductions of up to 50%. However, it is important to note that we observed a substantial increase in computational complexity when comparing HM to VTM. This complexity increase is not uniform and varies depending on factors such as QP values, frame rate, spatial texture, and motion. On the encoder side, our simultaneous profiling of both HM and VTM has identified additional intra modes and MTT partitioning as the primary factors responsible for the complexity increase in VTM. Additionally, on the decoder side, it was observed that ALF and DMVR represent the main sources of additional computational load in VTM compared to the HEVC decoding process.

#### REFERENCES

- [1] Gary J Sullivan, Jens-Rainer Ohm, Woo-Jin Han, and Thomas Wiegand, "Overview of the high efficiency video coding (hevc) standard," *IEEE Transactions on Circuits and Systems for Video Technology*, vol. 22, no. 12, pp. 1649–1668, 2012.
- [2] J. Ohm, G. J. Sullivan, H. Schwarz, T. K. Tan, and T. Wiegand, "Comparison of the coding efficiency of video coding standards including high efficiency video coding (hevc)," *IEEE Transactions on Circuits and Systems for Video Technology*, vol. 22, no. 12, pp. 1669–1684, Dec 2012.
- [3] T. K. Tan, R. Weerakkody, M. Mrak, N. Ramzan, V. Baroncini, J. Ohm, and G. J. Sullivan, "Video quality evaluation methodology and verification testing of hevc compression performance," *IEEE Transactions on Circuits and Systems for Video Technology*, vol. 26, no. 1, pp. 76–90, Jan 2016.
- [4] N. Sidaty, W. Hamidouche, O. Deforges, and P. Philippe, "Compression efficiency of the emerging video coding tools," in *2017 IEEE International Conference on Image Processing (ICIP)*, Sep. 2017, pp. 2996–3000.
- [5] J. Chen, E. Alshina, G. J. Sullivan, J.-R. Ohm, and J. Boyce, "Algorithm description of Joint Exploration Test Model 3 (JEM3)," in *Document JVET-C1001 3rd JVET Meeting*, Geneva, CH, May 2016.
- [6] J. Pfaff, H. Schwarz, D. Marpe, B. Bross, S. De-Luxán-Hernández, P. Helle, C. R. Helmrich, T. Hinz, W. Q. Lim, J. Ma, T. Nguyen, J. Rasch, M. Schäfer, M. Siekmann, G. Venugopal, A. Wiecekowski, M. Winken, and T. Wiegand, "Video compression using generalized binary partitioning, trellis coded quantization, perceptually optimized encoding, and advanced prediction and transform coding," *IEEE Trans. Circuits Syst. Video Technol.*, pp. 1–1, 2019.
- [7] Wassim Hamidouche, Thibaud Biatek, Mohsen Abdoli, Edouard François, Fernando Pescador, Miloš Radosavljević, Daniel Menard, and Mickael Raulet, "Versatile video coding standard: A review from coding tools to consumers deployment," *IEEE Consumer Electronics Magazine*, vol. 11, no. 5, pp. 10–24, 2022.
- [8] Alexandre Mercat, Florian Arrestier, Wassim Hamidouche, Maxime Pelcat, and Daniel Menard, "Energy reduction opportunities in an hevc real-time encoder," in *2017 IEEE International Conference on Acoustics, Speech and Signal Processing (ICASSP)*, 2017, pp. 1158–1162.
- [9] Y. J. Ahn, W. J. Han, and D. G. Sim, "Study of decoder complexity for HEVC and AVC standards based on tool-by-tool comparison," in *Applications of Digital Image Processing XXXV*, Andrew G. Tescher, Ed. International Society for Optics and Photonics, 2012, vol. 8499, pp. 327 – 340, SPIE.
- [10] W. Hamidouche, M. Raulet, and O. Deforges, "4k real-time and parallel software video decoder for multilayer hevc extensions," *IEEE Transactions on Circuits and Systems for Video Technology*, vol. 26, no. 1, pp. 169–180, Jan 2016.
- [11] F. Bossen, B. Bross, K. Suhring, and D. Flynn, "Hevc complexity and implementation analysis," *IEEE Transactions on Circuits and Systems for Video Technology*, vol. 22, no. 12, pp. 1685–1696, Dec 2012.
- [12] B. Bross, V. George, M. Alvarez-Mesa, T. Mayer, C. C. Chi, J. Brandenburg, T. Schierl, D. Marpe, and B. Juurlink, "Hevc performance and complexity for 4k video," in *2013 IEEE Third International Conference on Consumer Electronics - ICCE-Berlin (ICCE-Berlin)*, Sep. 2013, pp. 44–47.
- [13] W. Hamidouche, P. Philippe, C. Mohamed, A. Kammoun, D. Menard, and O. Deforges, "Hardware-friendly dst-vii/dct-viii approximations for the versatile video coding standard," in *2019 Picture Coding Symposium (PCS)*, 2019, pp. 1–5.
- [14] J. Chen Y. Ye and S-H. Kim, "Algorithm description for Versatile Video Coding and Test Model 5 (VTM 5)," in *document JVET-N1002, 14th JVET meeting*, Gothenburg, SE, Mar. 2019.
- [15] Xin Zhao, Jianle Chen, Marta Karczewicz, Amir Said, and Vadim Seregin, "Joint Separable and Non-Separable Transforms for Next-Generation Video Coding," *IEEE Transactions on Image Processing*, vol. 27, no. 5, pp. 2514–2525, May 2018.
- [16] W.-J. Chien, J. Boyce, Y.-W. Chen, R. Chernyak, K. Choi, R. Hashimoto, Y.-W. Huang, H. Jang, S. Liu, and D. Luo, "JVET AHG report: Tool reporting procedure (AHG13)," in *JVET document 00013 (JVET-00013), 15th JVET Meeting*, Gothenburg, SE, 2019.
- [17] B. Bross, J. Chen, and S. Liu, "Versatile Video Coding (Draft 5)," in *document JVET-N1001, 14th JVET meeting*, Geneva, CH, Mar. 2019.
- [18] Zhou Wang, A. C. Bovik, H. R. Sheikh, and E. P. Simoncelli, "Image quality assessment: from error visibility to structural similarity," *IEEE Trans. Image Process.*, vol. 13, no. 4, pp. 600–612, April 2004.
- [19] Mingliang Zhou, Xuekai Wei, Shiqi Wang, Sam Kwong, Chi-Keung Fong, Peter H. W. Wong, Wilson Y. F. Yuen, and Wei Gao, "SSIM-Based Global Optimization for CTU-Level Rate Control in HEVC," *IEEE Transactions on Multimedia*, vol. 21, no. 8, pp. 1921–1933, Aug. 2019.
- [20] Anne Aaron et al Zhi Li, "Toward A Practical Perceptual Video Quality Metric," in *Netflix TechBlog*, Berlin, Germany, June 2016.
- [21] G. Bjøntegaard, "Calculation of Average PSNR Differences Between RD-curves," in *VCEG-M33 ITU-T Q6/16*, Austin, TX, USA, Apr. 2001.
- [22] G. Bjøntegaard, "Improvements of the BD-PSNR Model," in *document VCEG-A111, ITU-T SG16/Q6, 35th VCEG Meeting*, Berlin, Germany, Jul. 2008.
- [23] ITU-T, "ITU-T Rec. P.910: Subjective Video Quality Assessment Methods for Multimedia Applications," Apr. 2008.
- [24] ITU-R, "ITU-R Rec. BT.500, ITU-R, Methodology for the Subjective Assessment of the Quality of Television Picture," Jan. 2012.
- [25] ITU, "Recommendation ITU-T P.910 : Subjective video quality assessment methods for multimedia applications," 1999.
- [26] F. Kozamernik, V. Steinman, P. Sunna, and E. Wyckens, "SAMVIQ A New EBU Methodology for Video Quality Evaluations in Multimedia," Amsterdam, IBC 2004, pp. 191–202.
- [27] ITU-R BT.1788, "Methodology for the Subjective Assessment of Video Quality in Multimedia Applications," 2007.
- [28] EBU BPN 056, "SAMVIQ Subjective Assessment Methodology for Video Quality," in *Report by EBU Project Group B/VIM (Video In Multimedia)*, May. 2003.
- [29] G. Gamst, L. Meyers, and A. Guarino, "Analysis of variance designs: A conceptual and computational approach with SPSS and SAS," in *Cambridge University Press*, New York, USA, 2008.
- [30] "Callgrind," <http://valgrind.org/docs/manual/cl-manual.html>.
- [31] Adam Wiecekowski, Jackie Ma, Heiko Schwarz, Detlev Marpe, and Thomas Wiegand, "Fast Partitioning Decision Strategies for The Upcoming Versatile Video Coding (VVC) Standard," in *2019 IEEE International Conference on Image Processing (ICIP)*, Taipei, Taiwan, Sept. 2019, pp. 4130–4134, IEEE.
- [32] Sik-Ho Tsang, Yui-Lam Chan, and Wei Kuang, "Mode Skipping for HEVC Screen Content Coding via Random Forest," *IEEE Transactions on Multimedia*, vol. 21, no. 10, pp. 2433–2446, Oct. 2019.
- [33] Liquan Shen and Guorui Feng, "Content-Based Adaptive SHVC Mode Decision Algorithm," *IEEE Transactions on Multimedia*, vol. 21, no. 11, pp. 2714–2725, Nov. 2019.
- [34] Tao Zhang, Ming-Ting Sun, Debin Zhao, and Wen Gao, "Fast Intra-Mode and CU Size Decision for HEVC," *IEEE Transactions on Circuits and Systems for Video Technology*, vol. 27, no. 8, pp. 1714–1726, Aug. 2017.
- [35] Sookyoung Ryu and Jewon Kang, "Machine Learning-Based Fast Angular Prediction Mode Decision Technique in Video Coding," *IEEE Transactions on Image Processing*, vol. 27, no. 11, pp. 5525–5538, Nov. 2018.

- [36] Hao Yang, Liqun Shen, Xinchao Dong, Qing Ding, Ping An, and Gangyi Jiang, "Low Complexity CTU Partition Structure Decision and Fast Intra Mode Decision for Versatile Video Coding," *IEEE Transactions on Circuits and Systems for Video Technology*, pp. 1–1, 2019.
- [37] Thomas Amestoy, Alexandre Mercat, Wassim Hamidouche, Cyril Bergeron, and Daniel Menard, "Random Forest Oriented Fast QTBT Frame Partitioning," in *ICASSP 2019 - 2019 IEEE International Conference on Acoustics, Speech and Signal Processing (ICASSP)*, Brighton, United Kingdom, May 2019, pp. 1837–1841, IEEE.
- [38] Wassim Hamidouche, Mickael Raulet, and Olivier Deforges, "4K Real-Time and Parallel Software Video Decoder for Multilayer HEVC Extensions," *IEEE Transactions on Circuits and Systems for Video Technology*, vol. 26, no. 1, pp. 169–180, Jan. 2016.
- [39] Benjamin Bross, Mauricio Alvarez-Mesa, Valeri George, Chi Ching Chi, Tobias Mayer, Ben Juurlink, and Thomas Schierl, "HEVC real-time decoding," San Diego, California, United States, Sept. 2013, p. 88561R.